Carbohydrate Polymers 136 (2016) 1348–1357

Contents lists available at ScienceDirect

Carbohydrate Polymers

journal homepage: www.elsevier.com/locate/carbpol

Determination of substitution positions in hyaluronic acid hydrogels using NMR and MS based methods

Frida J. Wende[a], Suresh Gohil[a], Hotan Mojarradi[b], Thibaud Gerfaud[c], Lars I. Nord[b], Anders Karlsson[b], Jean-Guy Boiteau[c], Anne Helander Kenne[b], Corine Sandström[a,*]

[a] Department of Chemistry and Biotechnology, Uppsala BioCenter, Swedish University of Agricultural Sciences, P.O. Box 7015, SE-750 07 Uppsala, Sweden
[b] Research A&C Galderma, Seminariegatan 21, SE-752 28 Uppsala, Sweden
[c] Galderma R&D, Les Templiers, 2400 route des Colles BP 87, 06410 Biot Cedex, France

ARTICLE INFO

Article history:
Received 10 May 2015
Received in revised form
25 September 2015
Accepted 30 September 2015
Available online 9 October 2015

Keywords:
Hyaluronic acid
Hydrogel
Cross-linked
Substitution
NMR
MS

ABSTRACT

In hydrogels of cross-linked polysaccharides, the total amount of cross-linker and the degree of cross-linking influence the properties of the hydrogel. The substitution position of the cross-linker on the polysaccharide is another parameter that can influence hydrogel properties; hence methods for detailed structural analysis of the substitution pattern are required.

NMR and LC–MS methods were developed to determine the positions and amounts of substitution of 1,4-butanediol diglycidyl ether (BDDE) on hyaluronic acid (HA), and for the first time it is shown that BDDE can react with any of the four available hydroxyl groups of the HA disaccharide repeating unit. This was achieved by studying di-, tetra-, and hexasaccharides obtained from degradation of BDDE cross-linked HA hydrogel by chondroitinase. Furthermore, amount of linker substitution at each position was shown to be dependent on the size of the oligosaccharides. For the disaccharide, substitutions were predominantly at ΔGlcA-OH2 and GlcNAc-OH6 while in the tetra- and hexasaccharides, it was mainly at the reducing end GlcNAc-OH4. In the disaccharide there was no substitution at this position. Since chondroitinase is able to completely hydrolyse non-substituted HA into unsaturated disaccharides, these results indicate that the enzyme is prevented to cleave on the non-reducing side of an oligosaccharide substituted at the reducing end GlcNAc-OH4. The procedure can be adopted for the determination of substitution positions in other types of polymers.

1. Introduction

Hydrogels formed by cross-linking of polysaccharides such as hyaluronic acid (HA, also known as hyaluronan) are materials that can be used for numerous applications, both medical and aesthetic (Burdick & Prestwich, 2011; Fakhari & Berkland, 2013; Gutowska, Jeong, & Jasionowski, 2001; Kogan, Šoltés, Stern, & Gemeiner, 2007; Schanté, Zuber, Herlin, & Vandamme, 2011). The hydrogels will have different physical properties depending on the starting material and the manufacturing process (Edsman, Nord, Öhrlund, Lärkner, & Kenne, 2012; Lapčík, Lapčík, De Smedt, Demeester, & Chabreček, 1998; Xu, Jha, Harrington, Farach-Carson, & Jia, 2012) and characterization of the chemical structure of the cross-linked network is essential for understanding and differentiating the different materials.

HA is a linear non-sulfated glycosaminoglycan built of the repeating unit disaccharide β-D-glucuronic acid-(1 → 3)-β-D-*N*-acetyl-D-glucosamine-(1 → 4). HA is present in all vertebrates and the primary structure is preserved through all species, the variation lying only in the molecular weight and polydispersity index of the polymer. In humans, HA is abundant in the skin, eyes and extracellular matrix (Laurent, 1987; Laurent & Fraser, 1992). Due to its numerous negative charges, HA can retain large amounts of water and acts therefore as a space filler, lubricant and osmotic buffer. However, the poor mechanical properties, rapid degradation

Abbreviations: HA, hyaluronic acid/hyaluronan; BDDE, 1,4-butanediol diglycidyl ether; BDPE, 1,4-butanediol di-(propan-2,3-diolyl)ether; DCM, dichloromethane; THF, tetrahydrofurane; TOCSY, total correlation spectroscopy; HSQC, heteronuclear single quantum correlation; NOESY, nuclear Overhauser effect spectroscopy; HMBC, heteronuclear multiple bond correlation; VCD, Vibrational circular dichroism.

* Corresponding author.
E-mail addresses: Frida.Wende@slu.se (F.J. Wende), Suresh.Gohil@slu.se (S. Gohil), Hotan.Mojarradi@galderma.com (H. Mojarradi), Thibaud.Gerfaud@galderma.com (T. Gerfaud), Lars.Nord@galderma.com (L.I. Nord), Anders.Karlsson@galderma.com (A. Karlsson), Jean-Guy.Boiteau@galderma.com (J.-G. Boiteau), Anne.HelanderKenne@galderma.com (A.H. Kenne), Corine.sandstrom@slu.se (C. Sandström).

http://dx.doi.org/10.1016/j.carbpol.2015.09.112

and clearance in vivo of soluble HA limit its use as a biomaterial. To improve the mechanical properties and to increase the resistance to degradation by hyaluronidases, HA is chemically modified or cross-linked to form hydrogels (Lapčík et al., 1998; Segura et al., 2005; Volpi, Schiller, Stern, & Šoltés, 2009).

A common procedure for cross-linking HA into hydrogels is the reaction with 1,4-butanediol diglycidyl ether (BDDE) under alkaline condition which yields a stable covalent ether linkage between HA and the cross-linker (Ågerup, Berg, & Åkermark, 2005). During the cross-linking process, the epoxide groups of BDDE react with nucleophiles forming derivatives of 1,4-butanediol di-(propan-2,3-diolyl)ether (BDPE). Some of the cross-linker molecules form true cross-links that are connected to HA at both ends while other BDDE molecules only bind at one end. Definitions of cross-linking parameters to describe the resulting HA hydrogels have been described in detail earlier (Kenne et al., 2013) as: (a) the degree of modification (MoD), which is the stoichiometric ratio between the sum of mono- and double-linked BDPE residues and HA disaccharide units; (b) the degree of substitution (DS) which is the proportion of the HA disaccharides that are substituted; (c) The degree of cross-linking (CrD), which is the stoichiometric ratio between BDPE residues that are double-linked and HA disaccharide units; (d) the effective cross-linker ratio (CrR), which is the fraction of cross-linker residues that are double-linked (forming cross-linkages in the polysaccharide network), compared to all linked cross-linkers.

The physical properties of the hydrogels can vary vastly depending on, e.g. the molecular weight of HA, the MoD and the cross-linking efficiency. Thus methods to differentiate HA gels on the molecular level are important to explain the different properties of the gels and also to understand the effect of different manufacturing processes used. Detailed structural analysis of intact HA hydrogels are however difficult due to the viscosity of the polymer and the complex cross-linked polymer network (Barbucci et al., 2006; Guarise, Pavan, Pirrone, & Renier, 2012; Pouyani, Harbison, & Prestwich, 1994). Recently, an analytical method that allows quantifying the MoD and CrD in cross-linked HA hydrogels was reported (Kenne et al., 2013). Using chondroitinase, a lyase which by an elimination reaction cleaves all 1,4-linkages between *N*-acetylglucosamine and glucuronic acid, HA is completely degraded into disaccharides with an unsaturated uronic acid at the non-reducing end (ΔHA_2, Fig. 1). When HA is substituted with BDPE, the cleavage is not complete and longer BDPE-substituted oligosaccharide fragments are generated. These oligosaccharides can be separated from the main non-substituted disaccharide (ΔHA_2) products by size-exclusion chromatography (SEC) and analyzed by electrospray ionization mass spectrometry (ESI-MS), allowing the determination of CrR (Kenne et al., 2013). The total amount of BDPE linked to HA, expressed as the MoD, can be determined by ^{1}H NMR spectroscopy. From these two parameters which give information about the polymer network, the DS and the CrD can be obtained (Kenne et al., 2013).

Besides MoD and CrD, the substitution positions for the BDPE-molecules on HA could also influence the properties of the hydrogel. In the reaction, nucleophilic groups of HA react with the epoxide groups of BDDE. In theory, six positions in each HA-disaccharide building blocks are available for reaction with BDDE, the hydroxyl groups, the carboxylate group and the amide group. The hydroxyl groups are the most likely binding positions as any esters formed with the carboxylate group of HA will probably be cleaved under the alkaline conditions used in the synthesis and the amide nitrogen has the lowest reactivity. The relative tendency of binding to the four different hydroxyl groups may vary due to steric differences between primary and secondary alcohols, conformational effects of the polymer due to hydrogen bonding and hydration (Nestor, Kenne, & Sandström, 2010), differences in pK_a of the hydroxyl groups and differences in reaction conditions during the manufacturing process. In this work, we have established NMR and LC–MS based methods to determine the position of substitution of mono-linked BDPE in oligosaccharides of different lengths obtained by enzymatic hydrolysis of cross-linked HA hydrogels.

2. Experimental

2.1. Materials

HA hydrogel cross-linked with BDDE was prepared under alkaline conditions and the HA concentration was adjusted to 20 mg/ml after neutralization. The MoD and CrR determined using the method by Kenne et al. (2013) were 8% and 0.1%, respectively. Chondroitinase ABC from *Proteus vulgaris* (art. no. C2905) was purchased from Sigma Aldrich.

2.2. Degradation and separation

The hydrogel (1 g in 100 ml 1 mM sodium phosphate buffer pH 7.0) was treated with chondroitinase ABC (10 UN) in a sealed flask at 37 °C for 90 h. The degradation was followed by analysing the sample on a Superdex Peptide 10/300 GL column (GE Healthcare, Uppsala, Sweden) using analytical HPLC with a diode-array detector (LC10vp LC system, Shimadzu). The degradation was considered complete when the viscosity of the sample was low, no remaining gel particles were observed and the sample contained mostly low-molecular weight oligosaccharides as demonstrated by HPLC–MS analysis (response for ΔHA_2 more than 70% out of 21 detected modified and unmodified oligosaccharides with size up to 16 monosaccharides). The enzyme digest was separated using preparative HPLC (ÄKTA purifier with UV-detector UV-900, pump P-900 and sample pump P-960, GE Healthcare, Uppsala, Sweden) in two steps. The first separation was performed by injecting 5 ml of the enzyme digest (sample pump, 5 ml/min) on to an in-house-packed Q Sepharose High Performance 16/170 column (GE Healthcare, Uppsala, Sweden) using a gradient of 1 mM sodium phosphate buffer pH 7.0 and 1 mM sodium phosphate buffer pH 7.0 with 200 mM sodium chloride (0–40% 43 min, 40% 6.5 min, 100% 9.5 min) at 5 ml/min. UV detection (232 nm) was used to monitor the separation and fractions were collected automatically according to predetermined limits of the UV-signal. The content of the collected fractions were analyzed with the Superdex Peptide 10/300 GL on the analytical HPLC. Fractions containing equal oligosaccharides were pooled and lyophilized. The obtained powder from the fractions containing ΔHA_2-B, ΔHA_4-B, ΔHA_6-B were dissolved in 10 ml of 100 mM ammonium acetate pH 7.8 and were then further purified from salt and other impurities on the ÄKTA purifier by injecting 1 ml with a sample loop on a self-packed Superdex Peptide Prep Grade 16/750 column (GE Healthcare, Uppsala, Sweden). Isocratic elution with 100 mM ammonium acetate pH 7.8 at 1.0 ml/min was used. UV detection (232 nm) was used to monitor the separation and fractions were collected automatically based on the UV-signal. The pure fractions containing ΔHA_2-B, ΔHA_4-B, ΔHA_6-B were analyzed with Superdex Peptide 10/300 GL on the analytical HPLC and then lyophilized. The fractions containing HA oligosaccharides at both ends of BDPE were also collected but not analyzed further.

2.3. NMR spectroscopy

The freeze dried di-, tetra- and hexasaccharide samples were dissolved in D_2O and transferred into either 5 or 3 mm NMR sample tubes. The NMR spectra were recorded either on a Bruker AVANCE^{TM} III 600 MHz spectrometer using a 5 mm PABBO BB/^{19}F-^{1}H/D Z-GRD probe or a 5 mm ^{1}H/^{13}C/^{15}N/^{31}P cryoprobe, both equipped with a z-gradient. All experiments were performed using

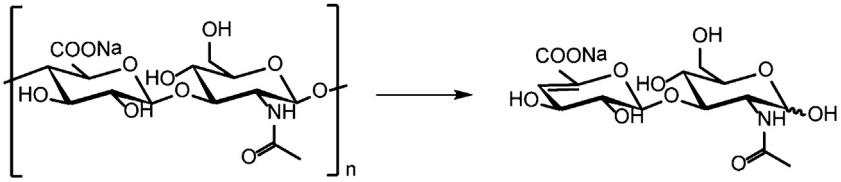

Fig. 1. ΔHA_2 formed by degradation of HA with chondroitinase ABC.

D_2O as solvent and the signals were referenced by adding a small portion of acetone-d_6 to the sample and setting the acetone-d_5 signal to δ_H 2.204. The temperatures were set between 280 and 300 K in order to get as little interference from the residual HDO peak as possible. The assignments of ^1H and ^{13}C resonances were obtained from homonuclear ^1H–^1H COSY, TOCSY and NOESY and heteronuclear ^1H–^{13}C HSQC, HSQC–TOCSY and HMBC experiments from the Bruker pulse sequence library. Mixing times from 10 to 120 ms were used for TOCSY spectra. Suppression of the water signal was achieved using the noesy pr1d pulse sequence. For quantification of amount of substitution by integration of NMR signals, the 1D ^1H NMR spectra were recorded with a recycle delay of 100 s. The ^1H NMR spectra of enantiomerically enriched (2′R,2″R)-BDDE were recorded on a Bruker Avance 400 MHz.

2.4. Mass spectrometry

All LC–MS analyses were performed on a Bruker Maxis Impact Mass spectrometer connected to an Agilent 1100LC system equipped with a diode-array UV detector. A Hypercarb™ column of dimension 100 mm × 4.6 mm and with particle size 3 μm (Thermo Scientific) was used and kept at 60 °C. The mobile phases were water and acetonitrile with 0.05 or 0.1% trifluoroacetic acid and the flow rate was 0.5 ml/min. A gradient of acetonitrile from 20 to 40% enabled a reasonable separation of isomers of ΔHA_2-B. UV absorbance was measured at 235 nm and the peak areas in the chromatogram were used to estimate the relative amounts of each isomer assuming that all isomers had the same response factors. For MS/MS, the technique of multiple reactions monitoring (MRM) was utilized. Whenever possible, direct infusion or flow injection analyses were used to optimize the collision energy to be used in CID. A collision energy of 45–50 eV was sufficient to give rise to cross-ring cleavages.

2.4.1. Reduction of HA oligomers

Since the column separates the α and β isomers, the hemiacetal form of the oligosaccharides were reduced to alditol using sodium borohydride in order to simplify the chromatographic peak profiles. The oligosaccharide fragments were dissolved in 200 μl of freshly prepared stock solution of 1 M NH_4OH containing 4 mg/ml of $NaBH_4$ and incubated at 40 °C for 30 min in a heating block. The reaction was quenched by adding 0.5 ml of 10% acetic acid in methanol followed by evaporation to dryness at 40 °C using a rotary evaporator. Addition of the acetic acid solution and evaporation was repeated two more times. The final evaporation was done using pure methanol. After the final evaporation, the residue was dissolved in H_2O:acetonitrile (80:20) before analysis.

2.5. Hydrolytic kinetic resolution of BDDE

To a stirred solution of (1S,2S)-(−)-1,2-cyclohexanediamino-*N*,*N*′-bis(3,5-di-t-butylsalicylidene)cobalt(II) (0.60 g; 0.99 mmol; 0.01 eq.) in 10 ml dichloromethane (DCM) at 23 °C acetic acid was added (566 μl; 9.89 mmol; 0.10 eq.) and the reaction mixture stirred at 23 °C under air for 30 min. Once the colour changed from red to dark brown (Co(II) to Co(III) oxidation) the reaction mixture was evaporated to dryness under vacuum. The catalyst was then dissolved in THF (20.0 ml) and racemic BDDE (18.2 ml; 98.9 mmol; 1.00 eq.) was added. The mixture was cooled down to 0 °C and water (1.43 ml; 79.1 mmol; 0.80 eq.) was added. The reaction mixture was allowed to warm up to 23 °C and stirred at this temperature for 24 h. After this time, the reaction mixture was evaporated to dryness. The dark red oil was purified two times by column chromatography on silica gel eluting with DCM and then with DCM/diisopropyl ether 85/15 to yield enantiomerically enriched (2′R,2″R)-BDDE (3.60 g; 18% yield) as a pale brown oil. ^1H NMR (400 MHz, DMSO-d_6): δ 3.67 (dd, J = 11.6, 2.8 Hz, 2H), 3.49–3.38 (m, 4H), 3.23 (dd, J = 11.5, 6.3 Hz, 2H), 3.09 (ddt, J = 6.9, 4.3, 2.8 Hz, 2H), 2.72 (dd, J = 5.2, 4.2 Hz, 2H), 2.54 (dd, J = 5.2, 2.7 Hz, 2H), 1.58–1.51 (m, 4H).

2.6. Derivatization of enantiomerically enriched BDDE for enantiopurity measurement

To a stirred solution of enantiomerically enriched (2′R,2″R)-BDDE (300 mg; 1.48 mmol; 1.00 eq.) in methanol (3.00 ml) at 0 °C was added 2-naphthalenethiol (0.48 g; 2.97 mmol; 2.00 eq.) followed by triethylamine (411 μl; 2.97 mmol; 2.00 eq.). The reaction mixture was stirred at 0 °C for 2 h and then allowed to warm up to 23 °C and stirred at this temperature for 18 h. The reaction mixture was filtered and the filtrate partitioned between DCM (50 mL) and water (50 mL). Phases were separated and the organic layer was washed with 1 M aqueous HCl (50 mL), dried over $MgSO_4$ and evaporated to dryness to yield the desired product (700 mg; 90% yield) as a colourless oil. ^1H NMR (400 MHz, DMSO-d_6): δ 7.88–7.75 (m, 8H), 7.53–7.38 (m, 6H), 5.18 (d, J = 5.3 Hz, 2H), 3.80 (h, J = 5.4 Hz, 2H), 3.46–3.32 (m, 8H), 3.21 (dd, J = 13.3, 5.2 Hz, 2H), 3.05 (dd, J = 13.3, 6.6 Hz, 2H), 1.57–1.40 (m, 4H). MS (m/z, ES^+): 545.2 ($[M+Na]^+$).

HPLC with a chiral column was recorded on an Agilent 1100 Series system using the following parameters: Column: Chiralpak ID 5 μm, 250 mm × 4.6 mm; Flow rate = 1.0 mL/min; 30.0 min runs; solvent system: heptane 65%, iPrOH 35%; isocratic flow. Chiral HPLC showed the following ratio: enantiomer 1 (t_R = 19.9 min): 5%; meso isomer (t_R = 22.8 min): 7%; enantiomer 2 (t_R = 26.2 min): 86%.

2.7. Determination of absolute configuration

A FTIR spectrometer (Vertex 70, Bruker) equipped with a vibrational circular dichroism (VCD) module (PMA 50, Bruker) for VCD measurements was used.

2.8. Computational methods

The density functional theory (DFT) calculations were carried out at 298 K in gas phase with Gaussian 09.

3. Results and discussion

3.1. Isolation of HA-BDPE fragments

The HA hydrogel formed by reaction with BDDE was degraded as previously described (Kenne et al., 2013), but using chondroitinase ABC instead of chondroitinase AC. The product mixture obtained

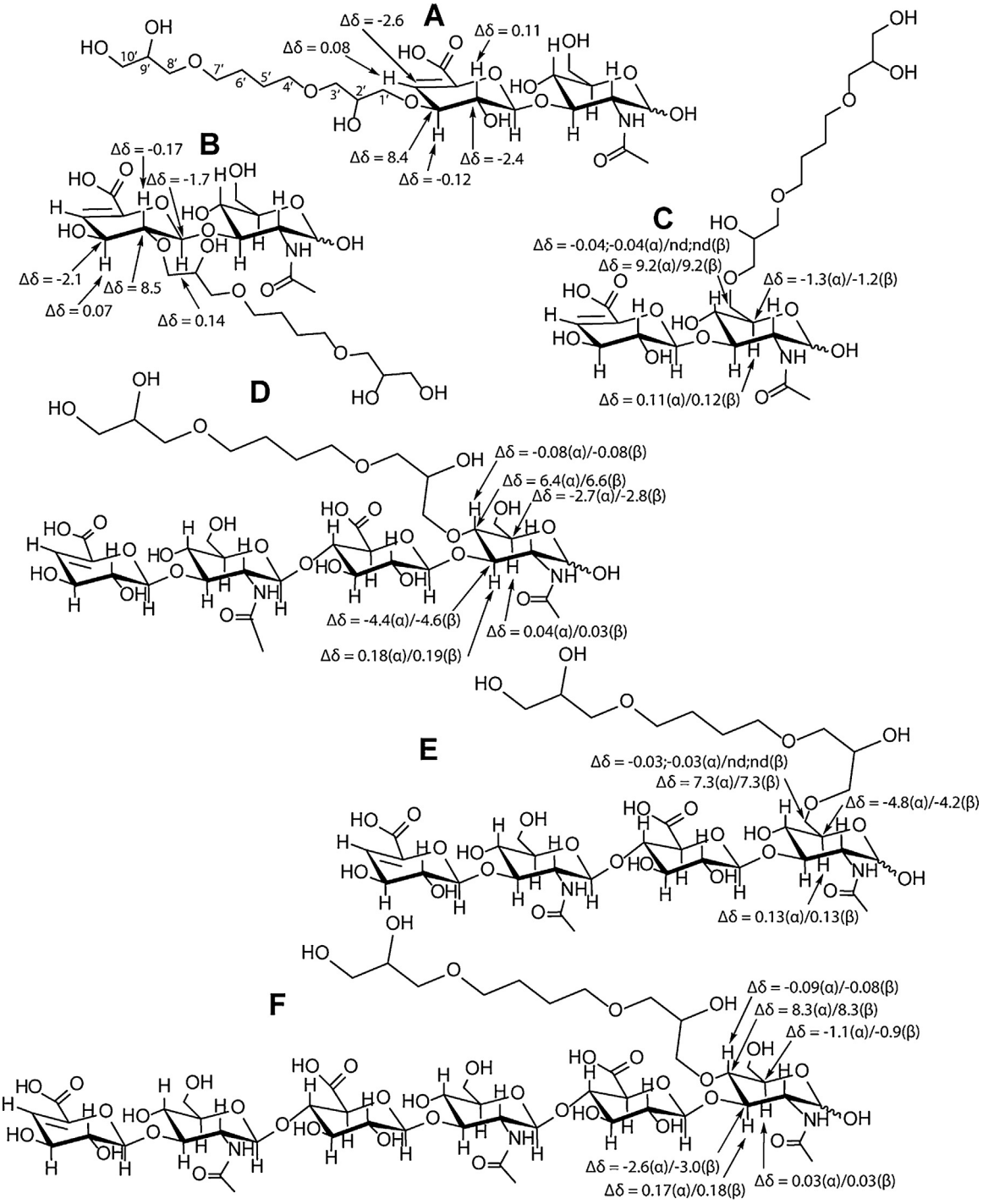

Fig. 2. Structures for the six oligosaccharides (A–F) identified from fractions ΔHA_2-B, ΔHA_4-B and ΔHA_6-B. $\Delta\delta$ values (ppm) show chemical shift differences compared to the unsubstituted oligosaccharides for the atoms closest to the substitution position. See Tables 1–3 for ^1H and ^{13}C chemical shifts.

after the enzymatic degradation was separated by anion exchange chromatography (Fig. 1 of supplementary material). The fractions corresponding to the monosubstituted di-, tetra- and hexasaccharides were collected for further analysis of the position of substitution by BDPE.

3.2. Nomenclature

The fragments obtained from enzymatic digestion with chondroitinase ABC are unsaturated HA oligosaccharides which are abbreviated ΔHA_x where x refers to the length of the oligosaccharide. The fragments with mono-linked BDPE which are investigated in this work are abbreviated as ΔHA_x-B. The monosaccharide residues within the chain are named ΔGlcA (unsaturated glucuronic acid), $GlcA_y$ (glucuronic acid), and $GlcNAc_y$ (*N*-acetyl glucosamine) where "*y*" indicates the position of the residue starting from the reducing end. The substitution positions are referred to as the monosaccharide residue together with the suffix -OHZ where "Z" is the position on the ring which is substituted.

Table 1
^{1}H and ^{13}C chemical shifts (ppm) of the resonances for the three substituted disaccharides (A–C) in ΔHA_2-B. Values in bold face indicate the position of substitution.

	Sugar residue	$^{1}H/^{13}C$							
		1	2	3	4	5	6	6′	Me
A	β-D-ΔGlcA-(1→	5.18	3.88	**4.05**	5.94	–	–	–	–
		100.4	67.4	**74.6**	104.7	144.3	169.1	–	–
	→3)-α-GlcNAc$_1$	5.16	4.05	4.05	3.53	3.90	3.83	3.83	2.13
		90.8	53.3	78.9	68.2	71.4	60.4	60.4	22.1
	→3)-β-GlcNAc$_1$	4.76	3.83	3.85	3.51	3.51	3.91	3.76	2.13
		94.4	55.9	81.1	68.2	75.6	60.6	60.6	22.1
B	β-D-ΔGlcA-(1→	5.34	**3.60**	4.24	5.89	–	–	–	–
		98.9	**78.3**	64.1	107.1	144.3	169.1	–	–
	→3)-α-GlcNAc$_1$	5.16	4.05	4.05	3.53	3.90	3.83	3.83	2.13
		90.8	53.3	78.9	68.2	71.4	60.4	60.4	22.1
	→3)-β-GlcNAc$_1$	4.76	3.83	3.85	3.51	3.51	3.91	3.76	2.13
		94.4	55.9	81.1	68.2	75.6	60.6	60.6	22.1
C	β-D-ΔGlcA-(1→	5.20	3.77	4.16	5.87	–	–	–	–
		100.5	69.7	66.0	107.1	144.3	169.1	–	–
	→3)-α-GlcNAc$_1$	5.16	4.07	4.01	3.58	4.02	**3.80**	**3.80**	2.13
		90.8	53.1	79.3	68.4	70.2	**69.7**	**69.7**	22.1
	→3)-β-GlcNAc$_1$	4.76	3.83	3.84	3.55	3.63	**nd**[a]	**nd**[a]	2.13
		94.4	55.8	81.5	68.3	74.3	**69.9**	**69.9**	22.1

[a] Could not be determined due to overlapping signals.

3.3. NMR analysis of fractions ΔHA_2-B, ΔHA_4-B and ΔHA_6-B

The ^{1}H and ^{13}C resonances were assigned from a combination of 1D and 2D NMR experiments including TOCSY, HSQC, HSQC-TOCSY, NOESY and HMBC and by comparison with the NMR spectra of HA oligosaccharides (Blundell, Reed, & Almond, 2006; Nestor et al., 2010). The substitution positions were determined based on changes in ^{1}H and ^{13}C chemical shifts ($\Delta\delta$) in the substituted oligosaccharides when compared to those in the unsubstituted oligosaccharides. Substitutions by BDPE cause an upfield shift of the proton signal attached to the carbon whose hydroxyl group is substituted by BDPE while the carbon experience a large downfield shift. Adjacent proton and carbon signals are also affected but in the opposite direction and to lesser extent.

3.3.1. Substitution positions in fraction ΔHA_2-B

In the fraction ΔHA_2-B, three types of disaccharides (named A–C, Fig. 2) with substitution by BDPE at three different positions, ΔGlcA-OH3 (A), ΔGlcA-OH2 (B) and GlcNAc$_1$-OH6 (C) were identified. Comparison of the ^{1}H and ^{13}C chemical shifts in ΔHA_2-B with those in the unsubstituted disaccharide ΔHA_2 showed large $\Delta\delta$ for H2/C2 and H3/C3 of ΔGlcA and for H6/C6 of GlcNAc (Fig. 2, Table 1). For example, the upfield shifts of H2 by ~0.17 ppm together with the downfield shift of C2 by ~8.5 ppm proved substitution by BDPE at this position. The neighbouring C1/H1 and C3/H3 showed opposite behaviour with C1 and C3 being slightly shielded while H1 and H3 were deshielded in good agreement with what is expected upon substitution on sugar rings. The same trends in chemical shift changes were observed for substitution at ΔGlcA-OH3 and at GlcNAc$_1$-OH6. A disaccharide with substitution by BDPE at GlcNAc$_1$-OH4 was not identified in the ΔHA_2-B fraction. The largest changes in chemical shifts compared to the unsubstituted disaccharide are shown in Fig. 2.

In solution, the GlcNAc sugar at the reducing end exists in equilibrium between the α- and β-anomeric forms in a 65/35% ratio. Thus, in the NMR spectra of ΔHA_2-B, two signals should be observed for all the protons on the reducing sugar as well as for all the protons on the non-reducing sugar due to the two anomeric forms of the reducing rings. However, because the anomeric configuration usually has a negligible influence on the conformation, the proton chemical shifts of the non-reducing units are very similar, and due to limited spectral resolution, only the protons on the reducing residue as well as the anomeric protons on the neighbouring sugars are usually clearly differentiated. Besides the observation of anomeric pairs of isomers, the oligosaccharides present in fraction ΔHA_2-B were also shown to exist as a mixture of diastereoisomers as demonstrated by the doubling of the signals in the NMR spectra (Fig. 3) and of the peaks in the LC–MS chromatograms (vide infra) originating from the use of racemic BDDE in the synthesis of the HA cross-linked gel.

The origin of the different types of isomers observed for ΔHA_2-B is clarified in Fig. 4. In fact, four diastereoisomers are expected to be formed after the reaction of HA with racemic BDDE: HA-(2′R,9′R)-BDPE, HA-(2′S,9′S)-BDPE, HA-(2′S,9′R)-BDPE and HA-(2′R,9′S)-BDPE (see Fig. 2 for BDPE atom numbering). The asymmetric carbon in position 9′, resulting from hydrolysis of the epoxide, is on a very flexible chain having minimal impact on column separation and NMR properties. Only the asymmetric carbon in position 2′, resulting from the sugar-reacted epoxide, is close enough to permit separation of the corresponding diastereoisomers on column chromatography and modify the NMR spectra.

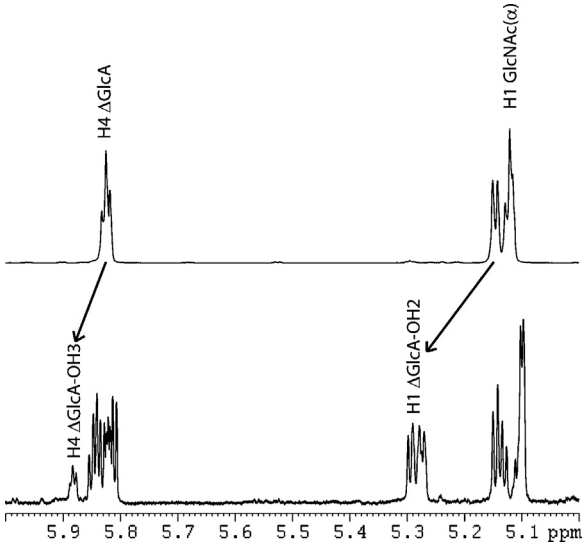

Fig. 3. Portion of the ^{1}H NMR spectra of (top) ΔHA_2 and (bottom) ΔHA_2-B showing the H4, H1 of ΔGlcA and the H1 of GlcNAc(α).

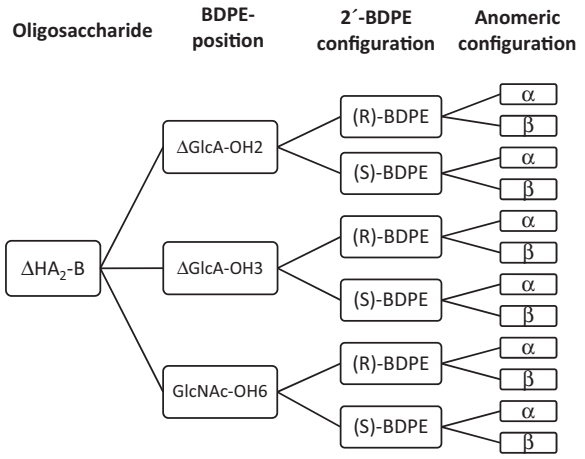

Fig. 4. Schematic representation of the different types of isomers observed in the NMR and LC–MS spectra of ΔHA_2-B.

Once the ^1H and ^{13}C chemical shifts of the different types of substituted disaccharides have been assigned from a combination of 2D NMR experiments, the position and amount of substitution at each position can be determined directly from the 1D ^1H NMR spectra. Indeed, it can be seen in Fig. 3 that the H1 and H4 signals of ΔGlcA experience a downfield shift upon substitution at the 2- and 3-position respectively and can be used as chemical shift reporters of substitution at these positions. Integration of these signals gave ~52% substitution at ΔGlcA-OH2 and ~13% at ΔGlcA-OH3. Since there is no substitution at $GlcNAc_1$-OH4, the anomeric signal of $GlcNAc_1$ integrates for the disaccharides with BDPE at ΔGlcA-OH2, ΔGlcA-OH3 and $\Delta GlcNAc_1$-OH6. Thus, integration of this signal gave ~35% of BDPE substitution at $GlcNAc_1$-OH6.

3.3.2. Substitution positions in fraction ΔHA_4-B

In the ΔHA_4-B fraction, four different types of tetrasaccharides were identified (the two most abundant are presented in Table 2, Fig. 2). The signals at δ_H 5.94 and δ_H 5.34 corresponding to H4 and H1 of ΔGlcA showed, by comparison with the assignments for ΔHA_2-B, that small amounts of tetrasaccharides substituted in positions ΔGlcA-OH2 and ΔGlcA-OH3 were present. The two other substituted tetrasaccharides (D and E) were present in larger amount and the ^1H and ^{13}C chemical shift values revealed that in both compounds, substitution occurred on the GlcNAc residue at the reducing end, one on $GlcNAc_1$-OH4 (D) and the other one on $GlcNAc_1$-OH6 (E) (Fig. 2). Tetrasaccharides with substitution by BDPE on the internal GlcNAc or GlcA sugars were not identified in the ΔHA_4-B fraction.

As for ΔHA_2-B, the positions of substitution by BDPE in ΔHA_4-B can be determined from the 1D ^1H NMR spectra and the amount quantified by integration of characteristic signals (Fig. 5): The H1 and H4 signals of ΔGlcA are used for determination of amount of substitution at ΔGlcA-OH2 and -OH3. The H1 signals of $GlcNAc_1$ in the α-anomeric form allow obtaining the amount of substitution at $GlcNAc_1$-OH4 while the H1 signals of $GlcNAc_1$ in the β-anomeric form give the sum of substitution at the $GlcNAc_1$-OH4 and -OH6 positions. Integration of these signals gave 72% substitution by BDPE at $GlcNAc_1$-OH4 and 21% at $GlcNAc_1$-OH6. The remaining two substitution positions contributed with less than 1% for ΔGlcA-OH3 and ca. 5–6% for ΔGlcA-OH2.

3.3.3. Substitution positions in the fraction ΔHA_6-B

Analysis of the NMR spectra of the ΔHA_6-B fraction showed that substitution by BDPE occurred almost exclusively at $GlcNAc_1$-OH4 on the reducing end (Table 3, Fig. 2). Hexasaccharides with BDPE substitution on ΔGlcA-OH2, ΔGlcA-OH3 and $GlcNAc_1$-OH6 were present in very small amounts (Table 4). Hexasaccharides with BDPE substitution on the internal sugars were not present in the ΔHA_6-B fraction.

Table 2
^1H and ^{13}C chemical shifts (ppm) of the resonances for the two most abundant substituted tetrasaccharides (D and E) in ΔHA_4-B. Values in bold face indicate the position of substitution.

	Sugar residue	$^1H/^{13}C$							
		1	2	3	4	5	6	6′	Me
D	β-ΔGlcA-(1→	5.17	3.76	4.16	5.86	–	–	–	–
		100.6	69.6	66.0	107.1	144.3	169.1	–	–
	→3)-β-$GlcNAc_3$-(1→	4.62	3.86	3.84	3.53	3.53	3.80	3.93	2.07
		100.5	54.5	81.7	68.1	75.3	60.3	60.3	22.3
	→4)-β-$GlcA_2$-(1→[a]	4.56	3.34	3.59	3.77	3.66	–	–	–
		103.4	72.5	73.4	80.4	76.5	173.7	–	–
	→4)-β-$GlcA_2$-(1→[b]	4.52	3.35	3.59	3.77	3.66	–	–	–
		103.4	72.4	73.5	80.4	76.5	173.7	–	–
	→3)-α-$GlcNAc_1$	5.11	4.06	4.09	**3.49**	3.92	3.84	3.84	2.03
		90.8	53.5	77.5	**76.9**	70.5	60.1	60.1	21.8
	→3)-β-$GlcNAc_1$	4.68	3.86	3.91	**3.46**	3.51	3.79	3.89	2.03
		94.5	56.0	79.7	**76.8**	74.6	60.1	60.1	22.2
E	β-ΔGlcA-(1→	5.17	3.75	4.16	5.86	–	–	–	–
		100.6	69.6	66.0	107.1	144.3	169.1	–	–
	→3)-β-$GlcNAc_3$-(1→	4.59	3.86	3.84	3.52	3.52	3.80	3.93	2.07
		100.2	54.5	81.9	68.1	75.4	60.3	60.3	22.3
	→4)-β-$GlcA_2$-(1→[a]	4.52	3.38	3.59	3.76	3.72	–	–	–
		102.9	72.4	73.4	79.8	76.2	174.0	–	–
	→4)-β-$GlcA_2$-(1→[b]	4.48	3.38	3.59	3.75	3.72	–	–	–
		102.9	72.2	73.4	79.8	76.2	174.0	–	–
	→3)-α-$GlcNAc_1$	5.16	4.06	3.92	3.60	4.01	**3.79**	**3.79**	2.03
		90.8	52.8	79.5	72.1	68.4	**69.7**	**69.7**	21.8
	→3)-β-$GlcNAc_1$	4.72	3.84	3.73	3.56	3.61	**nd**[c]	**nd**[c]	2.03
		94.6	55.3	82.0	68.2	73.2	**69.7**	**69.7**	22.2

[a] Connecting to reducing end GlcNAc in α configuration.
[b] Connecting to reducing end GlcNAc in β configuration.
[c] Could not be determined due to overlapping signals.

Table 3
^{1}H and ^{13}C chemical shifts (ppm) of the resonances for the most abundant substituted hexasaccharide (F) in ΔHA_6-B. Values in bold face indicate the position of substitution.

	Sugar residue	$^{1}H/^{13}C$							
		1	2	3	4	5	6	6′	Me
F	β-ΔGlcA-(1→	5.17	3.76	4.15	5.86	–	–	–	–
		100.5	69.6	65.8	107.0	144.3	169.2	–	–
	→3)-β-GlcNAc$_5$-(1→	4.58	3.86	3.83	3.51	3.51	3.79	3.93	2.07
		100.2	54.5	81.8	68.0	75.3	60.2	60.2	22.2
	→4)-β-GlcA$_4$-(1→	4.47	3.35	3.59	3.74	3.72	–	–	–
		103.0	72.2	73.3	79.7	76.0	174.2	–	–
	→3)-β-GlcNAc$_3$-(1→	4.58	3.85	3.72	3.54	3.49	3.79	3.92	2.03
		100.7	54.1	82.1	68.1	75.0	60.2	60.2	22.2
	→4)-β-GlcA$_2$-(1→[a]	4.56	3.34	3.58	3.76	3.65	–	–	–
		103.3	72.5	73.4	80.3	76.5	173.7	–	–
	→4)-β-GlcA$_2$-(1→[b]	4.51	3.33	3.58	3.75	3.64	–	–	–
		103.4	72.4	73.4	80.3	76.4	173.7	–	–
	→3)-α-GlcNAc$_1$	5.11	4.05	4.08	**3.48**	3.92	3.83	3.83	2.03
		90.8	53.5	77.5	**76.9**	70.3	60.0	60.0	21.8
	→3)-β-GlcNAc$_1$	4.67	3.84	3.89	**3.46**	3.51	3.78	3.92	2.03
		94.5	55.9	79.6	**76.8**	74.6	60.1	60.1	22.2

[a] Connecting to reducing end GlcNAc in α configuration.
[b] Connecting to reducing end GlcNAc in β configuration.

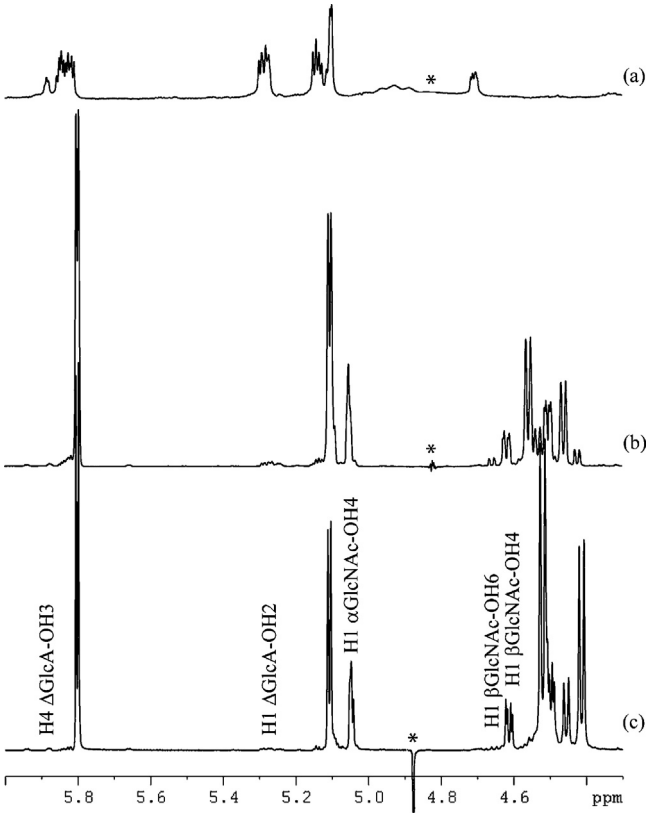

Fig. 5. Anomeric and H4 (ΔGlcA) region of the ^{1}H NMR spectra of (a) ΔHA_2-B, (b) ΔHA_4-B and (c) ΔHA_6-B. The NMR signals that can be used as reporters for identification and quantification of the position of substitution of BDPE on the sugars are indicated. *Residual HDO signal after water suppression.

Table 4
Amount (%) of substitution at the different positions in ΔHA_2-B, ΔHA_4-B and ΔHA_6-B obtained from integration of ^{1}H signals in NMR spectra and from areas of UV chromatograms.

Substitution position	ΔHA_2-B	ΔHA_4-B	ΔHA_6-B
ΔGlcA-OH2	52[a]/55[b]	6[a]/–[b]	~1[a]
ΔGlcA-OH3	13[a]/11[b]	<1[a]/–[b]	~1[a]
GlcNAc$_1$-OH4	–[a]/–[b]	72[a]/78[b]	92[a]
GlcNAc$_1$-OH6	35[a]/34[b]	21[a]/22[b]	~6[a]

[a] NMR.
[b] LC-UV; "–" not observed.

As for ΔHA_4-B, reporter signals that can be used for determination of amounts of substitution in ΔHA_6-B at the different positions are H1 and H4 of ΔGlcA for C2 and C3 substitution respectively, H1 of GlcNAc(α) for C4 substitution and H1 of GlcNAc(β) for C4 and C6 substitution (Fig. 5). Integration of the 1D ^{1}H NMR spectrum showed that more than 90% of the substitution occurs at GlcNAc$_1$-OH4.

3.3.4. Total distribution of BDPE in the oligosaccharides

Size-exclusion chromatography and NMR analysis revealed the distribution and position of BDPE in the oligosaccharide fractions obtained by enzymatic hydrolysis of the HA hydrogel. In the present example, ΔHA_6-B was the most abundant fraction (59%) collected by SEC followed by the ΔHA_4-B (26%) and ΔHA_2-B (15%) fractions (Table 5). In total in these three fractions, ca. 90% of substitution occurred on the GlcNAc residue at the reducing end and only 10% on the unsaturated non-reducing end ΔGlcA.

The fact that substitution occurred predominantly at GlcNAc$_1$-OH4 in ΔHA_6-B, while in ΔHA_4-B substitution was also found at GlcNAc$_1$-OH6 suggest that hydrolysis of the hexasaccharide by the enzyme did not proceed to completion during degradation of the gel. Indeed, addition of chondroitinase ABC in the NMR tube containing ΔHA_6-B followed by incubation at 37 °C resulted in further degradation of the hexasaccharide into the unsubstituted disaccharide ΔHA_2 and the tetrasaccharide ΔHA_4-B with BDPE at GlcNAc$_1$-OH4. No further hydrolysis of ΔHA_4-B was observed. Since the ΔHA_2-B fraction contains disaccharides substituted at ΔGlcA-OH2, ΔGlcA-OH3 and GlcNAc$_1$-OH6 but not at GlcNAc$_1$-OH4, it can be concluded that ΔHA_4-B with BDPE at GlcNAc$_1$-OH4 is not a substrate for the enzyme while the tetrasaccharides with

Table 5
Total distribution (%) of monosubstituted BDPE calculated from SEC and NMR data. The proportion of monosubstituted oligosaccharides (fraction of fragment) was obtained from SEC.

Fragment	Fraction of fragment (%)	ΔGlcA		GlcNAc$_1$	
		-OH2	-OH3	-OH4	-OH6
ΔHA_2-B	15	52	13	0	35
ΔHA_4-B	26	6	1	72	21
ΔHA_6-B	59	1	1	92	6
Total distribution of monosubstituted BDPE (%)		10	3	73	14

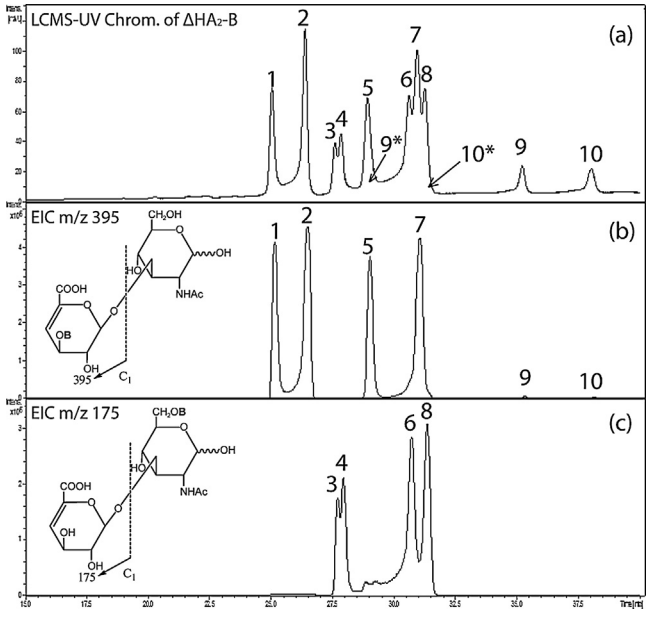

Fig. 6. LC-ESI–MS/MS of ΔHA_2-B in the negative ion mode: (a) UV chromatogram showing the 12 isomers that could be partially separated; (b) and (c) extracted ion chromatograms (EIC) of the glycosidic cleavage ions C_1, i.e. *m/z* 395 and *m/z* 175 indicating an attachment of BDPE on the ΔGlcA, and GlcNAc, respectively.

BDPE at other sugar positions can be further hydrolyzed by the enzyme.

3.4. LC–MS analysis of fractions ΔHA_2-B and ΔHA_4-B

3.4.1. Fraction ΔHA_2-B

A good separation of the disaccharides constituting the ΔHA_2-B fraction was achieved within a run time of 40 min using a porous graphite carbon based HPLC column. Analysis by LC-ESI–MS/MS in the negative ion mode showed the presence of twelve isobaric peaks (Fig. 6a). Since porous graphite carbon based columns are often able to resolve α- and β-anomers of carbohydrates, these twelve peaks were fractionated on an analytical scale and the partially pure fractions were, after lyophilization, injected once again into the LC–MS, one at a time. This caused additional peaks to appear in the chromatograms (data not shown) due to mutarotation occurring at the reducing-end $GlcNAc_1$ revealing the retention time of the other anomer. Hence the twelve peaks in Fig. 6a were confirmed to belong to six different isomers each one resolved as α- and β-anomeric pairs, namely peaks 1–2, 5–7, 3–6, 4–8, 9–9* and 10–10*, the anomers 9* and 10* being hidden under other peaks.

The MS/MS spectra of peaks 1 and 2 were, as expected, identical since these two peaks correspond to the α and β-anomeric pair. The MS/MS spectra of peaks 1 and 5 were also identical (see Fig. 2 of supplementary material) to the spectra of peaks 2 and 7 showing that substitution by BDPE at one position on the disaccharide gave

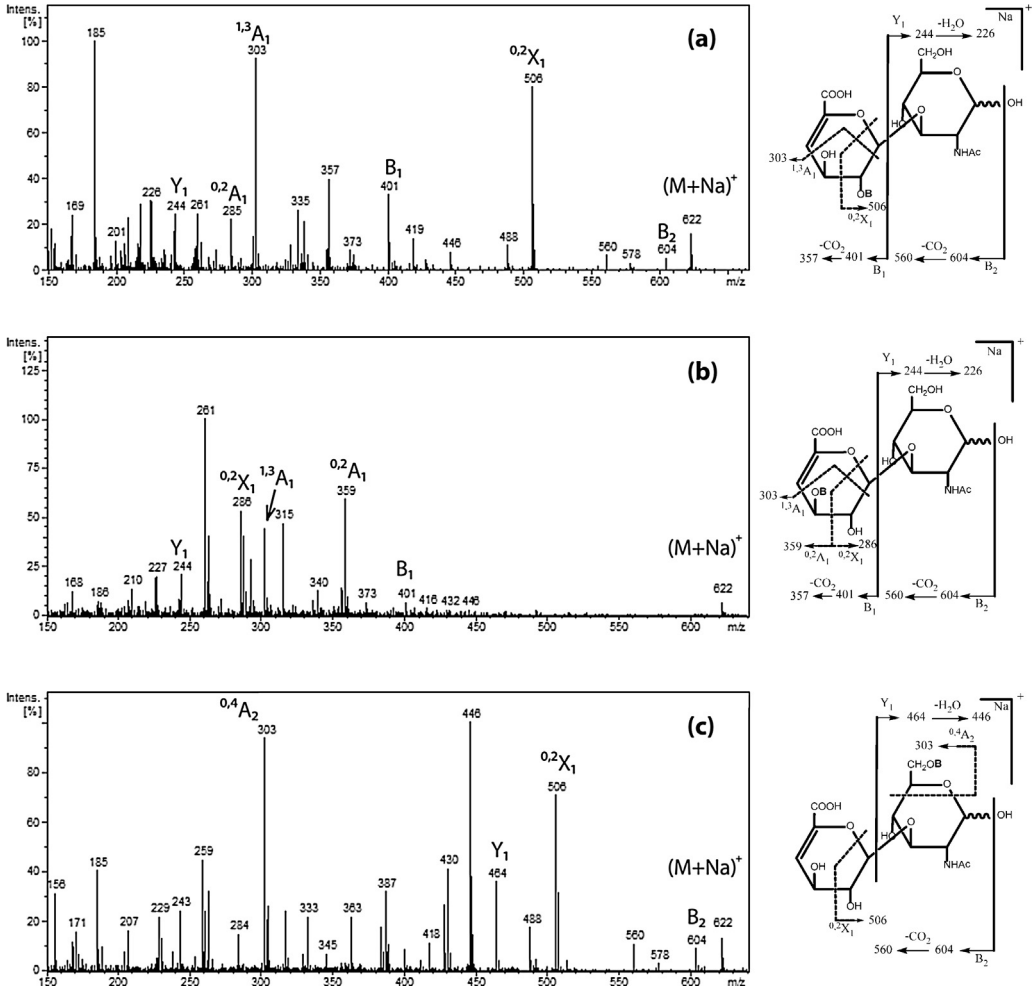

Fig. 7. ESI–MS/MS $[M+Na]^+$ spectra of peaks 1, 9 and 3 (from chromatogram a, Fig. 6) corresponding to BDDE at (a) ΔGlcA-OH2, (b) ΔGlcA-OH3 and (c) GlcNAc-OH6, respectively. The fragments are described using the nomenclature of Domon and Costello (1988). All the fragments are sodiated but Na is purposely excluded in the annotations above and in the text.

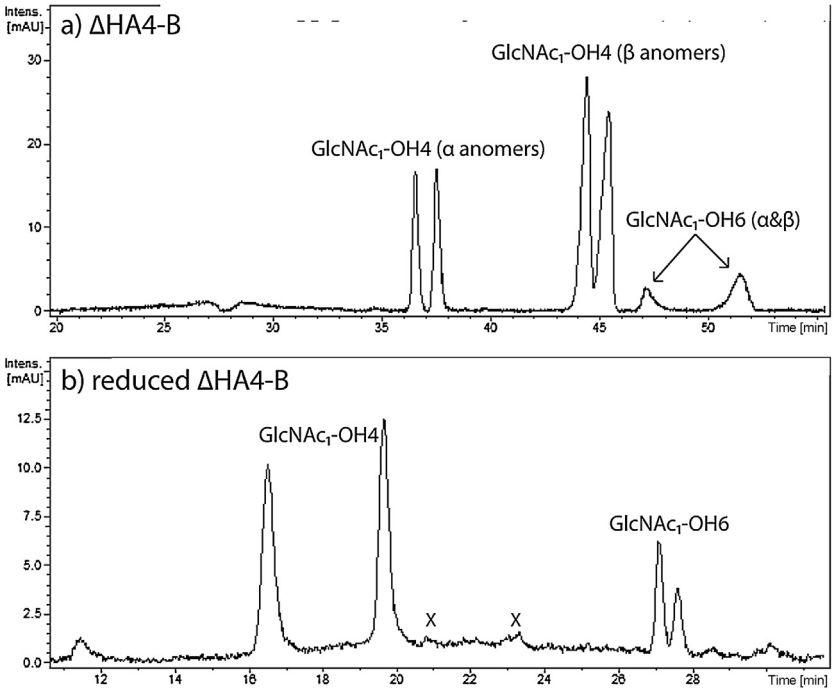

Fig. 8. (a) UV chromatogram (235 nm) from the LC–MS analysis of ΔHA_4-B. (b) UV chromatogram (235 nm) from the LC–MS analysis of borohydride reduced ΔHA_4-B showing the major substitutions at $GlcNAc_1$-OH4 and $GlcNAc_1$-OH6 of the two diastereoisomers. X denote minor components that appear as weak peaks in the extracted ion chromatogram of *m/z* 981, $[M+H]^+$, (data not shown). These peaks probably correspond to minor isomers with substitutions on ΔGlcA-OH2 and ΔGlcA-OH3 and represent approx. 5% of the total substitution.

rise to four peaks in the HPLC chromatogram, two of them originating from the α- and β-anomers. Reduction of fraction ΔHA_2-B using sodium borohydride in 0.1 M NH_4OH (see Section 2) followed by LC–MS analysis showed that the number of peaks decreased from twelve to six (see Fig. 3a of supplementary material), further confirming the existence of six α-,β-anomeric pairs of isomers in the fraction ΔHA_2-B.

The extracted ion chromatograms (EIC) of the glycosidic bond cleavage ion C_1, i.e. *m/z* 395 indicated that peaks 1, 2, 5 and 7 as well as peaks 9, 9*, 10 and 10* correspond to disaccharides with BDPE linked on ΔGlcA while *m/z* 175 indicated that peaks 3, 4, 6 and 8 represent a disaccharide with BDPE linked on GlcNAc (Fig. 6b and c).

From the peaks 1, 3 and 9 shown in the UV chromatogram (Fig. 6a), the position of substitution by BDPE was determined from MS/MS analysis in the positive ion mode of the precursor ion at *m/z* 622 ($[M+Na]^+$) (Fig. 7). The glycosidic cleavage fragments B and Y indicated on which sugars the BDPE molecule is attached while the cross-ring fragmentations, that involve rupturing two bonds on the same sugar residue, provided information on the linkage position of BDPE.

ΔGlcA-OH2 substitution was deduced from the diagnostic glycosidic cleavage ions B_1 at *m/z* 401 and Y_1 at *m/z* 244, Y_1–H_2O at *m/z* 226 indicating BDPE substitution on ΔGlcA and from the cross-ring ion $^{0,2}X_1$ at *m/z* 506 indicating BDPE substitution at ΔGlcA-OH2 (Fig. 7a). ΔGlcA-OH3 substitution was deduced from the diagnostic glycosidic cleavage ions B_1 at *m/z* 401 and Y_1 at *m/z* 244 indicating BDPE substitution on ΔGlcA and from the diagnostic cross-ring ions $^{0,2}X_1$ at *m/z* 286 and $^{0,2}A_1$ at *m/z* 359 indicating BDPE attachment on ΔGlcA-OH3 (Fig. 7b). ΔGlcNAc-OH6 substitution was deduced from the diagnostic glycosidic cleavage ions Y_1–H_2O at *m/z* 446 and from the diagnostic cross-ring ion $^{0,4}A_2$ at *m/z* 303 (Fig. 7c).

The relative amount of each isomer was obtained from the area under the peaks in the UV chromatogram of the reduced isomers and the data were in very good agreement with the data obtained by NMR (Table 4).

3.4.2. Fraction ΔHA_4-B

A total of eight peaks were detected for the ΔHA_4-B fraction (Fig. 8a) although not all of them could be resolved. As with ΔHA_2-B, when LC–MS was run on the reduced sample, only half the numbers of signals were present indicating the presence of two major diastereoisomers (Fig. 8b). These peaks were assigned as tetrasaccharides with BDPE substitution at C4 and C6 of $GlcNAc_1$ at the reducing end.

Since fraction ΔHA_6-B was shown by NMR to be further degraded by the enzyme into ΔHA_2 and ΔHA_4-B, it was not investigated by LC–MS.

3.5. Preparation of HA gel using enantiomerically enriched BDDE

NMR and LC–MS showed that the oligosaccharides present in fractions ΔHA_2-B, ΔHA_4-B and ΔHA_6-B exist as a mixture of diastereoisomers. To demonstrate that the diastereoisomers originated from the use of racemic BDDE in the synthesis of the HA cross-linked gel, enantiomerically enriched BDDE was prepared.

Hydrolytic kinetic resolution was used for the preparation of enantiomerically enriched BDDE from racemic BDDE (see Fig. 4 of supplementary material) (Schaus et al., 2002). Enantiomeric excess (ee) was determined using a chiral HPLC column after derivatization of enantiomerically enriched BDDE (see Fig. 5 of supplementary material) while the absolute configuration was obtained using VCD associated with density functional theory (DFT) calculations. The absolute configuration of this enantiomerically enriched BDDE was established to be (2′R,2′′R). (2′R,2′′R)-BDDE was then used to produce a HA hydrogel which was degraded and separated using the same experimental procedure as the one obtained with racemic BDDE.

LC–MS analysis of the ΔHA_2-B fraction obtained from the HA gel prepared with enantiomerically enriched BDDE showed that one of the two isomers of ΔGlcA-OH2, ΔGlcA-OH3 and GlcNAc-OH6 had decreased considerably in amount (see Fig. 3 of supplementary material). Similarly, the ^1H NMR spectra of the ΔHA_2-B fraction

obtained with (2′R,2″R)-BDDE clearly showed that H1 of ΔGlcA-OH2 now appeared as two doublets of relative intensities 65/35 representing the α- and β-anomeric forms of the disaccharide, thus consisting of only one HA-BDPE diastereoisomer (see Fig. 6 of supplementary material). The other two doublets that were slightly upfield shifted in the ΔHA_2-B fraction obtained from gel prepared with racemic BDDE were not present.

These data thus confirm that the additional signals observed in the NMR (see Fig. 6a of supplementary material) and LC–MS spectra (Fig. 6a) of ΔHA_2-B originating from HA-gel cross-linked with racemic BDDE are due to the diastereomeric mixture. Peaks 1 and 4 (Fig. 6) obtained from LC–MS analysis of ΔHA_2-B were collected and 1D ^{1}H NMR spectra were obtained for both of them. Peak 1 was shown to contain one diastereoisomer of the disaccharide substituted at ΔGlcA-OH2 (B) while peak 4 contained the other diastereoisomer (see Fig. 6 of supplementary material). As observed for the ΔHA_2-B fraction, the NMR spectrum of the ΔHA_4-B fraction from (2′R,2″R)-BDDE showed that only one diastereoisomer of the substituted tetrasaccharides was present (see Fig. 7 of supplementary material).

4. Conclusion

In this study, the position and amount of BDPE substitution in di-, tetra- and hexasaccharides from enzyme degraded hydrogel of cross-linked hyaluronic acid have been determined by NMR and LC–MS. The data obtained from both methods are in excellent agreement. In ΔHA_2-B, ΔHA_4-B and ΔHA_6-B, the substitution with BDPE is located on the hydroxyl group at the terminal reducing or non-reducing sugar residue. Substitution is either on $GlcNAc_1$-OH4/6 or on ΔGlcA-OH2/3 but does not occur on the internal sugar residues. In the ΔHA_2-B fraction, substitution in three of the four possible substitution positions is found. Substitution occurs predominantly at ΔGlcA-OH2 (>50%) and $GlcNAc_1$-OH6 (>30%). No disaccharide with substitution at $GlcNAc_1$-OH4 was identified. In the ΔHA_4-B and ΔHA_6-B fractions, substitution with BDPE was predominantly at $GlcNAc_1$-OH4 at the reducing end (>70% in ΔHA_4-B and >90% in ΔHA_6-B). The fact that the larger oligosaccharides are predominantly substituted at $GlcNAc_1$-OH4 while such substitution is not observed in the disaccharide indicates that tetrasaccharides with $GlcNAc_1$-OH4 substitution are not substrates for chondroitinase ABC. Diagnostic glycosidic cleavage and cross-ring ions that established the position of substitution in ΔHA_2-B by LC–MS and ^{1}H and ^{13}C NMR signals that can be used as chemical shifts reporters of the position of substitution of BDPE on the sugars of HA were also identified. The NMR and LC–MS methodologies presented in this work are not restricted to the study of HA gels made by reaction with BDDE but could also be adopted for other types of cross-linked HA hydrogels as well as other types of substituted polysaccharides that can be degraded enzymatically.

Acknowledgement

The authors thank Jean-Valère Naubron from the Spectropole of the Aix-Marseille University for the VCD measurements.

Appendix A. Supplementary data

Supplementary material associated with this article can be found, in the online version, at doi:10.1016/j.carbpol.2015.09.112.

References

Ågerup, B., Berg, P., & Åkermark, C. (2005). Non-animal stabilized hyaluronic acid – A new formulation for the treatment of osteoarthritis. *Biodrugs*, *19*(1), 23–30.
Barbucci, R., Leone, G., Chiumiento, A., Di Cocco, M. E., D'Orazio, G., Gianferri, R., et al. (2006). Low- and high-resolution nuclear magnetic resonance (NMR) characterisation of hyaluronan-based native and sulfated hydrogels. *Carbohydrate Research*, *341*(11), 1848–1858.
Blundell, C. D., Reed, M. A. C., & Almond, A. (2006). Complete assignment of hyaluronan oligosaccharides up to hexasaccharides. *Carbohydrate Research*, *341*(17), 2803–2815.
Burdick, J. A., & Prestwich, G. D. (2011). Hyaluronic acid hydrogels for biomedical applications. *Advanced Materials*, *23*(12), H41–H56.
Domon, B., & Costello, C. E. (1988). A systematic nomenclature for carbohydrate fragmentations in Fab-Ms Ms spectra of glycoconjugates. *Glycoconjugate Journal*, *5*(4), 397–409.
Edsman, K., Nord, L. I., Öhrlund, A., Lärkner, H., & Kenne, A. H. (2012). Gel properties of hyaluronic acid dermal fillers. *Dermatologic Surgery*, *38*(7), 1170–1179.
Fakhari, A., & Berkland, C. (2013). Applications and emerging trends of hyaluronic acid in tissue engineering, as a dermal filler and in osteoarthritis treatment. *Acta Biomaterialia*, *9*(7), 7081–7092.
Guarise, C., Pavan, M., Pirrone, L., & Renier, D. (2012). SEC determination of cross-link efficiency in hyaluronan fillers. *Carbohydrate Polymers*, *88*(2), 428–434.
Gutowska, A., Jeong, B., & Jasionowski, M. (2001). Injectable gels for tissue engineering. *Anatomical Record*, *263*(4), 342–349.
Kenne, L., Gohil, S., Nilsson, E. M., Karlsson, A., Ericsson, D., Kenne, A. H., et al. (2013). Modification and cross-linking parameters in hyaluronic acid hydrogels – Definitions and analytical methods. *Carbohydrate Polymers*, *91*(1), 410–418.
Kogan, G., Šoltés, L., Stern, R., & Gemeiner, P. (2007). Hyaluronic acid: A natural biopolymer with a broad range of biomedical and industrial applications. *Biotechnology Letters*, *29*(1), 17–25.
Lapčík, L., Jr., Lapčík, L., De Smedt, S., Demeester, J., & Chabreček, P. (1998). Hyaluronan: Preparation, structure, properties, and applications. *Chemical Reviews*, *98*(8), 2663–2684.
Laurent, T. C. (1987). Biochemistry of hyaluronan. *Acta Oto-Laryngologica*, (Suppl. 442), 7–24.
Laurent, T. C., & Fraser, J. R. E. (1992). Hyaluronan. *FASEB Journal*, *6*(7), 2397–2404.
Nestor, G., Kenne, L., & Sandström, C. (2010). Experimental evidence of chemical exchange over the beta(1 -> 3) glycosidic linkage and hydrogen bonding involving hydroxy protons in hyaluronan oligosaccharides by NMR spectroscopy. *Organic and Biomolecular Chemistry*, *8*(12), 2795–2802.
Pouyani, T., Harbison, G. S., & Prestwich, G. D. (1994). Novel hydrogels of hyaluronic-acid – Synthesis, surface-morphology, and solid-state NMR. *Journal of the American Chemical Society*, *116*(17), 7515–7522.
Schanté, C. E., Zuber, G., Herlin, C., & Vandamme, T. F. (2011). Chemical modifications of hyaluronic acid for the synthesis of derivatives for a broad range of biomedical applications. *Carbohydrate Polymers*, *85*(3), 469–489.
Schaus, S. E., Brandes, B. D., Larrow, J. F., Tokunaga, M., Hansen, K. B., Gould, A. E., et al. (2002). Highly selective hydrolytic kinetic resolution of terminal epoxides catalyzed by chiral (salen)Co-III complexes. Practical synthesis of enantioenriched terminal epoxides and 1,2-diols. *Journal of the American Chemical Society*, *124*(7), 1307–1315.
Segura, T., Anderson, B. C., Chung, P. H., Webber, R. E., Shull, K. R., & Shea, L. D. (2005). Crosslinked hyaluronic acid hydrogels: A strategy to functionalize and pattern. *Biomaterials*, *26*(4), 359–371.
Volpi, N., Schiller, J., Stern, R., & Šoltés, L. (2009). Role, metabolism, chemical modifications and applications of hyaluronan. *Current Medicinal Chemistry*, *16*(14), 1718–1745.
Xu, X., Jha, A. K., Harrington, D. A., Farach-Carson, M. C., & Jia, X. Q. (2012). Hyaluronic acid-based hydrogels: From a natural polysaccharide to complex networks. *Soft Matter*, *8*(12), 3280–3294.